A Low Cost Utility Interactive Inverter for Residential Fuel Cell Generation

Sangmin Jung, Youngsang Bae, Sewan Choi, *Senior Member, IEEE*, and Hyosung Kim, *Member, IEEE*

***Abstract*—This paper presents the development of a single-phase utility-interactive inverter for residential power generation to meet the specifications laid down for the 2005 Future Energy Challenge Competition sponsored by U.S. DOE and IEEE.**

The proposed inverter system is capable of working in both stand-alone and grid-connected mode. A control scheme for implementing both modes of operation is presented, which has simple structure with smaller number of sensors. The proposed control algorithm including the whole system control is implemented on a low cost, fixed-point DSP TMS320F2812. The experimental results from a 1 kW prototype show that the proposed inverter system exhibits not only low THD grid current during the grid-connected mode and well regulated inverter voltage during the stand-alone mode, but also smooth and automatic transfer between the two modes of operation.

***Index Terms*—Fuel cell, Future Energy Challence Competition, grid-connected, LCL filter, $P+$ resonant, stand-alone, utility-interactive inverter.**

I. Introduction

UTILITY interactive inverters converting dc power sources such as photovoltaics or fuel cells to ac grid systems are increasingly becoming popular as the energy crisis and environmental concern become the driving force for alternative energy. In general, the inverters employed in the small distributed generation is required to have the following characteristics: 1) allowable for wide output voltage variation of distributed energy sources; 2) assured output power quality with low THD and voltage/current flickering as well as frequency deviation; and 3) available for isolated operation and line parallel operation. In addition to these requirements, the inverter cost must also decrease while at the same time increasing efficiency, reliability, and power quality levels. The cost reduction of the inverters will enable the small distributed generation system to penetrate rapidly into the utility market and to provide load flexibility to bring significant lifestyle enhancements to remote areas in the developing world [1]. There have been many researches on three-phase grid-tie inverters [2]–[4], but few studies have been undertaken on a single-phase utility-interactive inverter capable of working in both grid- connected and stand-alone mode.

This paper presents the development of a single-phase utility-interactive inverter for residential power generation to meet the specifications laid down for the 2005 Future Energy Challenge Competition sponsored by U.S. DOE and IEEE. The inverter should be able to work grid-connected at unity power factor and stand-alone providing power for a resistive load. The inverter must be efficient and comply with requirements for harmonic control, interconnection and safety standards according to IEEE1547.

Manuscript received July 11, 2006; revised September 5, 2006. Recommended for publication by Associate Editor R. Teodorescu.

The authors are with the Seoul National University of Technology, Department of Control and Instrumentation Engineering, Seoul 139-743, Korea (e-mail: schoi@snut.ac.kr; hyoskim@kongju.ac.kr).

Digital Object Identifier 10.1109/TPEL.2007.909191

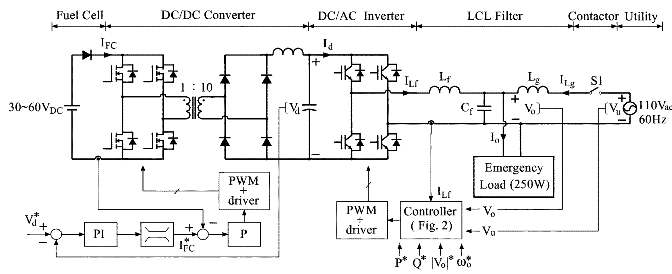

Fig. 1. Proposed utility interactive inverter system.

The proposed utility-interactive inverter has the following features.

- The inverter is operated in both grid-connected and stand-alone mode, and switching between the two modes is shown to be smooth and automatic.
- The proposed ac current and voltage control schemes show high performance and simple structure with smaller number of sensors.
- The proposed control scheme including the whole system control is implemented on a low cost, fixed point DSP TMS320F2812.
- The proposed single-phase inverter is suitable for utility-interactive residential power generation.

The control scheme is presented to implement both modes of operation. The mode transfer strategy for the proposed scheme is provided. The LCL filter design is detailed. Finally, the experimental results from a 1 kW prototype are presented to verify the effectiveness of the proposed control scheme.

II. Proposed Utility Interactive Inverter

A. System Configuration

Fig. 1 shows the configuration of the proposed utility interactive inverter system consisting of a distributed energy source, a dc-dc converter, a dc-ac inverter with a LCL filter, a static transfer switch, and an emergency load. The inverter should be able to supply a continuous 1 kW power from a dc voltage varying from 30 V to 60 V to a single-phase utility line of 110 V 60 Hz. The distributed energy source could be fuel cells or solar cells, and in this paper the design and control will be based on fuel cell application.

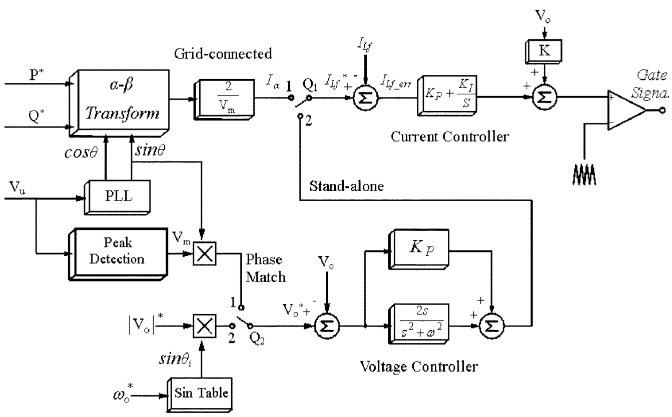

Fig. 2. DC-AC inverter control diagram for utility-interactive operation.

The dc-dc converter converts a unregulated voltage to a regulated 220 VDC. The full-bridge type is a topology of choice with which a phase-shift PWM technique can be implemented to achieve zero voltage switching, reducing turn-on loss of the switch. A PI compensator is used for the voltage control. A current control is also implemented to improve the dynamic characteristic of the system and to reduce current ratings of the power components during load transient condition. The single-phase dc-ac inverter converts a 220 VDC to a regulated 110 VAC 60 Hz. An output LCL filter is employed to reduce the ripple components due to PWM switching operation and draw a low THD ac waveform in the utility.

Static transfer switch "S1" is used to disconnect and reconnect the inverter output to the grid. When switch "S1" is closed, which is so called grid-connected mode, the inverter is operated in the current-controlled mode and current I_{Lf} is controlled to regulate the demanded power at unity power factor. In case of utility interruption or abnormal grid condition switch "S1" is open, which is so called stand-alone mode, the inverter is operated in the voltage-controlled mode and V_o is controlled to regulate the required output voltage across the emergency load.

B. Inverter Control for Utility Interactive Operation

Fig. 2 shows a control block diagram for the proposed utility-interactive inverter system. In the grid-connected mode control switch Q1 is connected to "1" and in the stand-alone mode control switch Q1 is connected to "2". A P+Resonant controller has been adopted for inverter output voltage in the stand-alone mode to reduce the steady-state error, and a inner current loop has been used to increase the dynamic performance during the transient state since the current loop acts as an "active damper" during the transient state such as a sudden load variation [12]. The inner current control loop with a voltage feed-forward has good performance when the grid voltage is distorted by low order harmonics. The inner current loop has also been used for grid current in the grid-connected mode, therefore an additional controller for grid current is not needed.

In the grid-connected mode, inverter current reference $I_{\mathrm{Lf}}*$ is obtained from the commanded power as shown in Fig. 2. The commanded real power P and reactive power Q are transformed into α axis current I_α which becomes inverter current reference $I_{\mathrm{Lf}}*$ and β axis current in the stationary reference frame as shown below [5]

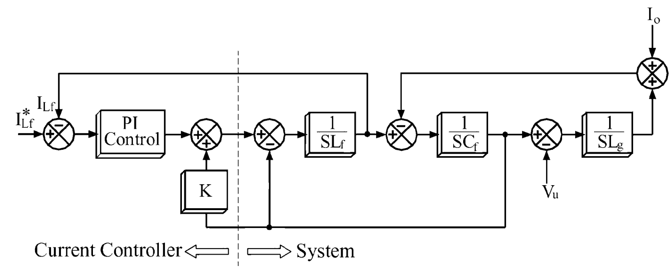

Fig. 3. System block diagram for current control.

$$\begin{bmatrix} I_\alpha \\ I_\beta \end{bmatrix} = \begin{bmatrix} V_\alpha & V_\beta \\ -V_\beta & V_\alpha \end{bmatrix}^{-1} \begin{bmatrix} P \\ Q \end{bmatrix} = \frac{2}{V_m} \cdot \begin{bmatrix} \sin\theta & -\cos\theta \\ \cos\theta & \sin\theta \end{bmatrix} \begin{bmatrix} P \\ Q \end{bmatrix} \tag{1}$$

where $V_\alpha = V_m \sin\theta$ and $V_\beta = V_m \cos\theta$, and V_m and θ is the magnitude and phase angle of the grid voltage generated from PLL block, respectively. An output voltage feed- forward is implemented to eliminate the steady-state error and improve the transient characteristics. Fig. 3 shows the system block diagram for current control with the output voltage feed-forward.

The transfer function of reference-to-actual inverter current can be obtained from Fig. 3 by

$$\frac{I_{\mathrm{Lf}}(s)}{I^*_{\mathrm{Lf}}(s)} = \frac{\mathrm{BS}^3 + \mathrm{CS}^2 + K_p S + K_I}{\mathrm{AS}^4 + \mathrm{BS}^3 + \mathrm{DS}^2 + K_p S + K_I} \tag{2}$$

where

$$A = L_f C_f L_g, B = K_P C_f L_g,$$
$$C = K_I C_f L_g, D = C + L_f + L_g - \mathrm{KL}_g.$$

With $\mathrm{K} = 1$ the transfer function (2) can be simplified as

$$\frac{I_{\mathrm{Lf}}(s)}{I^*_{\mathrm{Lf}}(s)} = \frac{C_f K_P S + C_f K_I}{L_f C_f S^2 + C_f K_P S + C_f K_I}. \tag{3}$$

The magnitude gain at the grid frequency ω_o becomes,

$$\frac{I_{\mathrm{Lf}}(j\omega_o)}{I^*_{\mathrm{Lf}}(j\omega_o)} \approx 1. \tag{4}$$

This is because the first term in the denominator of (3) becomes $-L_f C_f \omega_o^2 = -(\omega_o/\omega_r)^2 << 0$ since the grid frequency ω_o is much smaller than the resonant frequency $\omega_r = 1/\sqrt{L_T C_f}$, where $L_T = L_f \| L_g$. That is, it means that the steady state error at the grid frequency could be zero without regard to the system parameters. If $\mathrm{K} = 0$, the error depends on the system parameters such as K_I and C_f as we can see from (2). Also, the digital implementation of a PI control with a voltage feed-forward may cause an instability problem related to the filter delay or control time delay if the sampling frequency of the DSP is comparatively low, and therefore the sampling

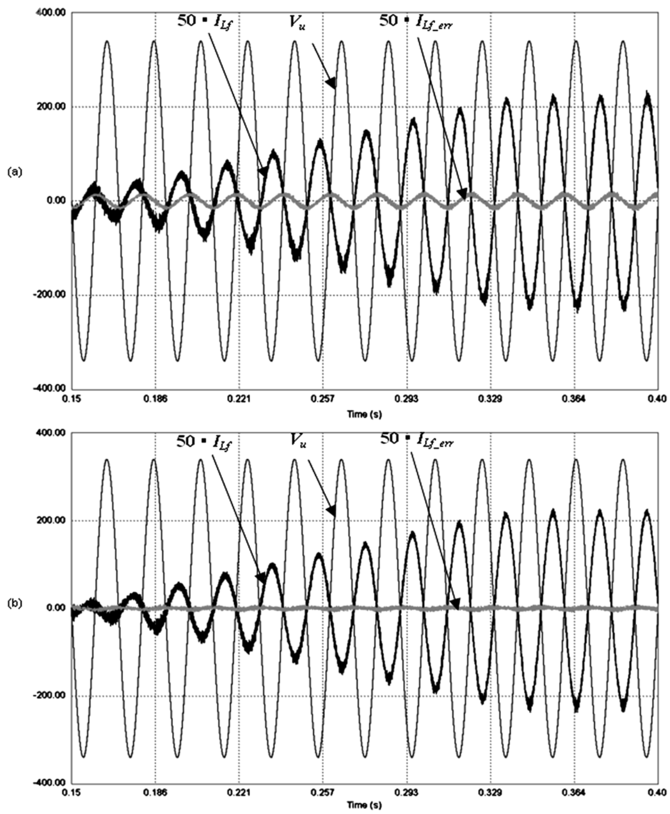

Fig. 4. Simulated waveforms showing steady-state and transience response of proposed current control. (a) Without the feed-forward control. (b) With the feed-forward control.

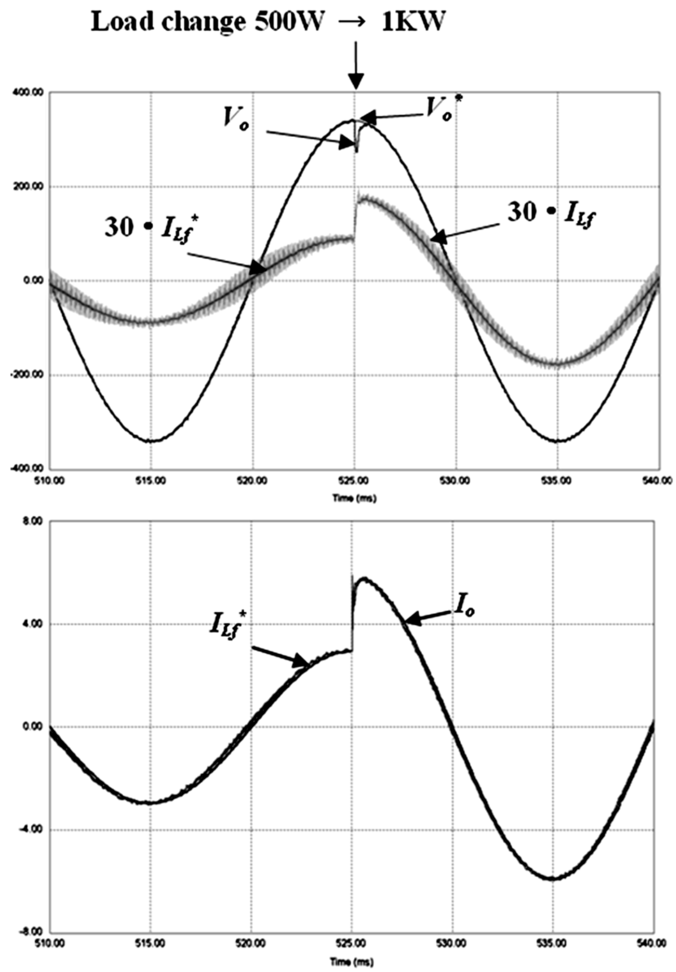

Fig. 5. Simulated waveforms showing steady-state and transience response of proposed voltage control.

frequency should be chosen high enough to avoid instability problem.

Fig. 4 shows the validity of the proposed current control method with the output voltage feed-forward in the grid-connected mode. The grid current is being ramping up to the rated value of 1 kW. It can be seen that there exist both steady-state and transient errors without the output voltage feed-forward. The elimination of both steady-state and transient errors can be clearly seen with the output voltage feed-forward.

In the stand-alone mode, a double-loop control of outer-loop voltage control and inner-loop current control is performed. Also, control switch Q2 is connected to "2" so that inverter voltage reference V_o* is obtained from a self-generated signal which is independent of the grid voltage.

During the stand-alone mode an ac voltage regulation should be performed, but the conventional PI regulator in the stationary frame can not eliminate steady-state errors due to finite gain at a frequency of the grid voltage [6]. A synchronous frame PI regulator can achieve zero steady error by shifting the ac quantities at a frequency of the grid voltage to dc quantities in the rotating reference frame so that the conventional PI regulator can be used. However, this synchronous frame PI regulator is complicated and computationally expensive especially in single-phase system due to the following reasons [7]; • A fictitious orthogonal phase is required for single-phase system. • Transformation of ac quantities in the stationary frame into dc quantities in rotating frame and *vice versa* is required. • The cross-coupling terms should be considered. Therefore, it is a burden for a low cost fixed point DSP controller such as TMS320F240 to implement the synchronous frame PI regulator along with the whole system control algorithm.

The P+Resonant regulator is shown to have zero steady state errors in the stationary frame and stable and good transient performance [8]. Fig. 5 shows the steady-state and transient response of the proposed voltage control method employing the P+Resonant regulator. It can be seen that there is no steady-state error during continuous modulation and only a little error at a step load change. Control switch Q2 is connected to "2" only except during a transfer from stand-alone mode to grid-connected mode at which switch Q2 is connected to "1" so that the inverter output voltage matches the grid voltage both in magnitude and phase before switch S1 is turned on and the grid-connected mode begins.

C. *Mode Transfer Strategy*

The utility-interactive inverter is required to switch seamlessly between the current control for the grid-connected mode and the voltage control for the stand-alone mode so that the operation ensures a smooth voltage profile across the load to avoid inrush currents and a smooth current profile into the grid to avoid voltage spikes [9].

Transfer From Grid-Connected Mode to Stand-Alone Mode: Assume the inverter is operating in the current-controlled mode with switch S1 closed. When a fault on the grid occurs, the grid voltage begins to drop or swell. The fault detection circuitry gives a turn off signal to S1 when the grid voltage is out of the normal operating voltage range. If an attempt to switch the inverter to voltage-control mode is made before S1 is actually turned off (A triac is essentially turned off when the current through it goes zero) abnormal voltage across inductors may occur due to large current through the capacitor resulting in failure of voltage control for stand-alone mode operation. Therefore, the transfer from grid-connected mode to stand-alone mode should be performed in the following sequence.

1) Detect a fault on the grid.
2) Give a turn off signal to switch S1.
3) Switch the inverter to voltage-control mode at the next zero crossing with voltage reference being measured from inverter output voltage V_o.
4) Gradually increase the voltage reference to the desired value.

Transfer From Stand-Alone Mode to Grid-Connected Mode: Assume the inverter is operating in the voltage- controlled mode with switch S1 open. When a fault on the grid is cleared and the grid voltage comes back on within the normal operating voltage range, the phase and magnitude of the grid voltage and the inverter output voltage may not match. The inverter is operated to adjust the inverter output voltage to match the grid voltage. If S1 is closed before the match occurs, abnormal current on inductor L_g may occur due to large voltage across the inductor resulting in failure of current control for grid-connected mode operation. Therefore, the transfer from stand-alone mode to grid-connected mode should be performed in the following sequence.

1) Detect that the grid voltage is within the normal operating voltage range.
2) Adjust the phase and magnitude of the inverter output voltage to match the grid voltage.
3) If the inverter output voltage matches the grid voltage, turn on switch S1 at the next zero crossing.
4) Switch the inverter to current-control mode with current reference being measured from inverter output current I_{Lf}.
5) Gradually increase the current reference to the desired value.

D. LCL Filter Design

A LCL filter is adopted in the proposed inverter system since it has advantages over a *LC* filter: First, it has better attenuation than a *LC* filter given the same size. Second, a LCL filter provides inductive output at the grid interconnection point to prevent inrush current [10].

- The base values can be calculated as,

$$R_b = \frac{V^2}{P} = 12.1\Omega \tag{5}$$

$$C_b = \frac{1}{\omega_o R_b} = 219.2uF \tag{6}$$

Where V is the output line-to-line rms voltage and P is the rated output power. The selection of filter capacitance C_f is a trade-off between reactive power in C_f and equivalent inductance L_T. Filter capacitance C_f should be limited by the amount of reactive power absorbed in the capacitor [11]

$$C_f = xC_b = 0.01 \times 219.2\,uF = 2.192\,uF \tag{7}$$

where x is the percentage of the reactive power absorbed in the rated condition and is set to be 1% in this paper.

- The filter resonance frequency f_r is determined to be 1.5 kHz which is one tenth of the inverter switching frequency ω_{sw}. Then, equivalent inductor L_T can be obtained by

$$L_T = \frac{1}{C_f}\left(\frac{1}{2\pi f_r}\right)^2 = 5.14\,mH. \tag{8}$$

- The current ripple on the grid-side inductor at the switching frequency should be attenuated with respect to the current ripple on the equivalent inductance. To obtain the desired current ripple attenuation of 20%, the following equation should be satisfied [11]

$$\frac{I_{\mathrm{Lg}}(h_{\mathrm{sw}})}{I_{\mathrm{LT}}(h_{\mathrm{sw}})} = \frac{1}{|1 + L_g(1/L_T - C_b\omega_{\mathrm{sw}}^2)|} = 20\%. \tag{9}$$

Therefore, from (9) the grid-side inductance becomes $L_g = 570.6\,uH$, resulting in $L_f = 4.57\,mH$.

III. Experimental Results

A 1 kW prototype inverter has been built, and experimental waveforms are presented in this section. The parameters used in the experiment are given by: • Input voltage : 30–60 VDC • dc link voltage : 220 VDC • Nominal grid voltage V_u : 110 V at 60 Hz • Nominal grid current I_{Lg}: 2.73A (300 W) • External load : 24.2 Ω (500 W) • Emergency load : 48.3 Ω (250 W).

Fig. 6 shows the experimental waveforms for a transfer from grid-connected mode to stand-alone mode. It can be seen from Fig. 6(a) that initially the inverter is injecting a current into the grid at unity power factor. Right after the grid voltage drops to 80 V which is out of the normal operating voltage range, a turn-off signal is applied to S1. The switch actually turns off at the next zero crossing of grid voltage (at the trigger position). As shown in Fig. 6(b), the inverter output voltage to which the emergency load is connected is shown to have no interruption at the time of turning off S1 and switching from current control to voltage control. Also, the inverter output voltage is being slowly ramped up to the rated value.

Fig. 7 shows the experimental waveforms for a transfer from stand-alone mode to grid-connected mode. The inverter is feeding the emergency load. It can be seen from Fig. 7(a) that right after the grid voltage comes back on to the nominal voltage of 110 V the inverter starts adjusting to match the phase and magnitude of the inverter output voltage to the grid voltage. The phase mismatch of the inverter output voltage and grid voltage decreases to zero in four cycles. Also, as shown in Fig. 7(b) switch S1 is turned on at the zero crossing (at the trigger position) after the match process, and grid current I_{Lg} start increasing slowly to the rated value. The measured THD

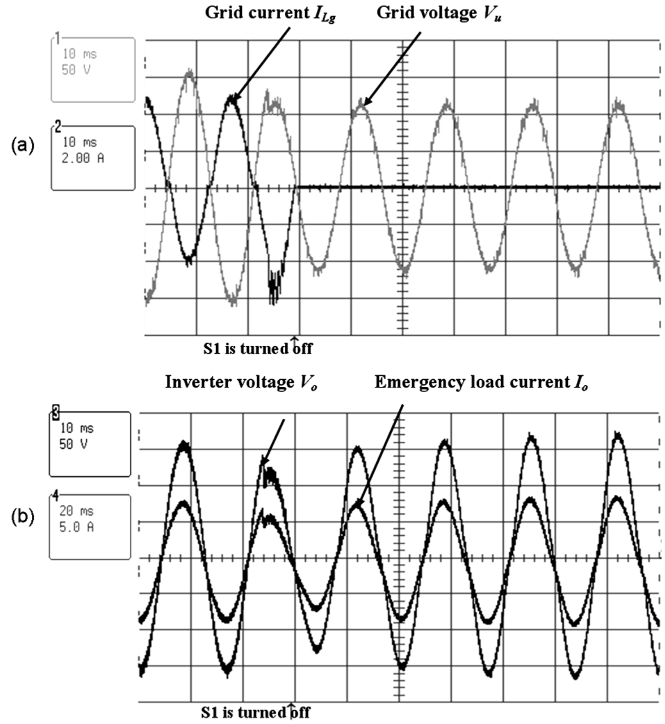

Fig. 6. Experiment waveforms during a transition from grid-connected mode to stand-alone mode.

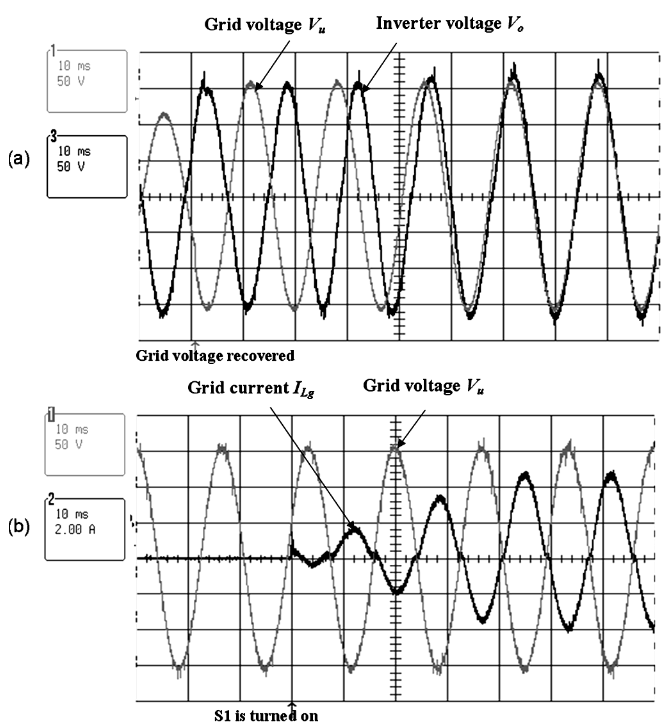

Fig. 7. Experiment waveforms during a transition from stand-alone mode to grid-connected mode. [Fig. 7(b) was measured several cycles after Fig. 7(a).]

of the grid current at the grid-connected mode and the inverter output voltage at the stand-alone-mode were 3.35% and 3.82%, respectively. The 2005 FEC specifications and the achieved experimental performance of SNUT team are listed in Table I. Photograph of the SNUT utility-interactive inverter system is shown in Fig. 8.

TABLE I
2005 FEC SPECIFICATIONS AND EXPERIMENTAL PERFORMANCE OF SNUT TEAM PROTOTYPE

Design Item		2005 FEC Specification performance	SNUT team Experimental performance
Frequency		60Hz ± 1.2Hz(2%)	59.85Hz~60.15Hz
Output voltage regulation		± 10%	-5.4%~+3.2%
THD	Output voltage harmonic	Lower than 5%	Lower than 3.82%
	Output Current harmonic	Lower than 5%	Lower than 3.35%
Power factor		Higher than 90%	Higher than 99%
Efficiency		Higher than 90%	Total 87% (DC-DC: 92%, INV:95%)

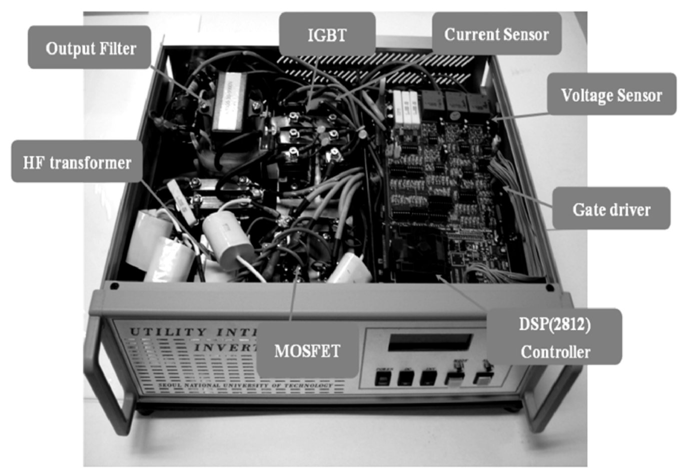

Fig. 8. Photograph of the SNUT utility-interactive inverter system.

IV. CONCLUSION

In this paper the development of a single-phase utility-interactive inverter for residential power generation is presented. A control scheme with simple structure has been proposed to implement both grid-connected and stand-alone modes of operation. The proposed control scheme including the system control has been implemented on a fixed point DSP TMS320F2812.

It has been shown from the experimental results that the proposed inverter system exhibits not only low THD grid current during the grid-connected mode and well regulated inverter voltage during the stand-alone mode, but also smooth and automatic transfer between the two modes of operation. The proposed inverter is suitable for single-phase utility-interactive residential power generation.

REFERENCES

[1] Y. Xue, L. Chang, S. B. Kjaer, J. Bordonau, and T. Shimizu, "Topologies of single-phase inverters for small distributed power generators: An overview," *IEEE Trans. Power Electron.*, vol. 19, no. 5, pp. 1305–1314, Sep. 2004.

[2] T. and D. G. Holmes, "Grid current regulation of a three-phase voltage source inverter with an LCL input filter," *IEEE Trans. Power Electron.*, vol. 18, no. 3, pp. 888–895, May 2003.

[3] M. Prodanovic and T. C. Green, "Control and filter design of three-phase inverters for high power quality grid connection," *IEEE Trans. Power Electron.*, vol. 18, no. 1, pp. 373–380, Jan. 2003.

[4] Q. Zeng and L. Chang, "Study of advanced current control strategies for three-phase grid-connected pwm inverters for distributed generation," in *Proc. IEEE Conf. Control Appl.*, Aug. 2005, pp. 1311–1316.

[5] H. Akagi and A. Nabae, "Control strategy of active power filters using multiple voltage-source PWM converter," *IEEE Trans. Ind. Electron.*, vol. IE-22, no. 3, pp. 460–465, May/Jun. 1986.
[6] X. Yuan, W. Merk, H. Stemmler, and J. Allmeling, "Stationary-frame generalized integrators for current control of active power filters with zero steady-state error for current harmonics of concern under unbalanced and distorted operating conditions," *IEEE Trans. Ind. Appl.*, vol. 38, no. 2, pp. 523–532, Mar. 2002.
[7] N. Zmood and D. N. Holmes, "Stationary frame current regulation of PWM inverters with zero steady-state error," *IEEE Trans. Power Electron.*, vol. 18, no. 3, pp. 814–822, May. 2003.
[8] M. Newman, "Design and control of a universal custom power conditioner," Ph.D. dissertation, Monash University, Victoria, Australia, 2002.
[9] R. Tirumala, N. Mohan, and A. Walter, "Seamless transfer of grid-connected PWM inverters between utility-interactive and stand-alone modes," in *Proc. Appl. Power Electron. Conf. Expo*, Dallas, TX, Mar. 2002, vol. 2, pp. 1081–1086.
[10] T. Wang, Z. Ye, G. Sinha, and X. Yuan, "Output filter design for a grid-interconnected three-phase inverter," in *Proc. 34th Annu. IEEE Appl. Power Electron. Conf. Expo. (PESC'03)*, Jun. 2003, vol. 2, pp. 779–784.
[11] M. Liserre, F. Blaabjerg, and S. Hansen, "Design and control of an lcl-filter based three-phase active rectifier," in *Proc. IEEE Ind. Appl. Conf.*, 2001, pp. 297–307.
[12] H. Kim and S.-K. Sul, "Compensation voltage control in dynamic voltage restorers by use of feed forward and state feedback scheme," *IEEE Trans. Power Electron.*, vol. 20, no. 5, pp. 1169–1177, Sep. 2005.
[13] M. Ciobotaru, R. Teodorescu, and F. Blaabjerg, "Control of single-stage single-phase PV inverter," in *Proc. IEEE 11th Eur. Conf. Power Electron. Appl.*, Dresden, Germany, Sep. 2005, p. 10.
[14] Z. Yao, Z. Wang, L. Xiao, and Y. Yan, "A novel control strategy for grid-interactive inverter in grid-connected and stand-alone modes," in *Proc. Appl. Power Electron. Conf. Expo (APEC'06)*, Mar. 2006, p. 5.
[15] R. Teodorescu and F. Blaabjerg, "Flexible control of small wind turbines with grid failure detection operating in stand-alone and grid-connected mode," *IEEE Trans. Power Electron.*, vol. 19, no. 5, pp. 1323–1332, Sep. 2004.
[16] A. V. Timbus, M. Ciobotaru, R. Teodorescu, and F. Blaabjerg, "Adaptive resonant controller for grid-connected converters in distributed power generation systems," in *Proc. Appl. Power Electron. Conf. Expo (APEC'06)*, Mar. 2006, p. 6.
[17] I. Hwang, K. Ahn, H. Lim, and S. Kim, "A control method and test results of utility-interactive photovoltaic power generation systems," *J. Korean Inst. Power Electron.*, vol. 5, pp. 123–129, Apr. 2000.
[18] T. Lee, S. Jang, J. Kim, J. Gu, C. Won, and C. Kim, "A study on PWM converter/inverter drive system by a fuel cell simulator," *J. Korean Inst. Power Electron.*, vol. 9, pp. 222–230, Jun. 2004.

Sangmin Jung was born in Seoul, Korea, in 1979. He received the B.S. and M.S. degrees from the Department of Control and Instrumentation Engineering, Seoul National University of Technology, Seoul, Korea, in 2004 and 2006, respectively.

He is currently an Engineer with the Research and Development Center, Hyosung Heavy Industries, Seoul. His research interests include power converter control and power conditioning system for fuel cells.

Mr. Jung received the 1st place and the 2nd place awards from the International Future Energy Challenge sponsored by the U.S Department of Energy, in 2003 and 2005, respectively.

Youngsang Bae was born in Kunsan, Korea, in 1979. He received the B.S. degree in electrical engineering from Hoseo University, Asan, Korea, in 2003 and the M.S. degree from the Department of Control and Instrumentation Engineering, Seoul National University of Technology, Seoul, Korea, in 2005.

He is currently an Engineer of the Research and Development Center, Power Plaza Industries, Seoul. His research interests include utility interface and power quality issues including power factor correction.

Sewan Choi (S'92–M'96–SM'04) received the B.S. degree in electronic engineering from Inha University, Incheon, Korea, in 1985 and the M.S. and Ph.D. degrees in electrical engineering from Texas A&M University, College Station, in 1992 and 1995, respectively.

From 1985 to 1990, he was with Daewoo Heavy Industries as a Research Engineer. From 1996 to 1997, he was a Principal Research Engineer at Samsung Electro-Mechanics Co., Korea. In 1997, he joined the Department of Control and Instrumentation Engineering, Seoul National University of Technology, Seoul, Korea, where he is currently an Associate Professor. He directed a student team to design and build a 10 KW fuel cell inverter for residential applications, which won the 1st place award in the 2003 Future Energy Challenge Competition sponsored by U.S. Department of Energy. His research interests include three-phase power factor correction, power conversion technologies in renewable energy systems, and dc-dc converters for hybrid electric and fuel cell vehicles.

Dr. Choi is an Associate Editor of the IEEE TRANSACTIONS ON POWER ELECTRONICS.

Hyosung Kim (S'90–M'96) received the B.S. and M.S. degrees in electrical engineering from Seoul National University, Seoul, Korea, in 1981 and 1983, respectively, and the Ph.D. degree from Chungbuk National University in 1995.

From 1982 to 1986, he was employed at Tong-Yang Cement Mfg. Co., Korea, where he participated in the factory automation and energy saving project. From 1996 to 1997, he was a visiting scholar in the Department of Electrical Engineering, Okayama University, Japan. From 2000 to 2001, he was an Associate Research Professor in the Institute of Energy Technology at Aalborg University, Denmark. Since 1997, he has been a tenured Professor in the School of Electrical and Electronics Engineering, Kongju National University, Korea. He is interested in power quality, static compensators, renewable energy, and line interactive inverters.